Technological University Dublin
ARROW@TU Dublin

Articles

School of Chemical and Pharmaceutical Sciences

2015

# Synthesis and Structural Characterizations of Ansa-Vanadabis(tricarbadecaboranyl) Sandwich Complexes

Ariane Perez-Gavilan
ariane.perezgavilan@tudublin.ie

Patrick J. Carroll
*University of Pennsylvania, Philadelphia, PA*

Larry Sneddon
*University of Pennsylvania, Philadelphia, PA*

Follow this and additional works at: https://arrow.tudublin.ie/scschcpsart

## Recommended Citation

Perez-Gavilan, A., Carroll, P.J., & Sneddon, L.G. (2015) Synthesis and structural characterizations of ansa-vanadabis (tricarbadecaboranyl) sandwich complexes. *Journal of Organometallic Chemistry,* 798 (2015): 263-267. doi.org/10.1016/j.jorganchem.2015.04.002

This Article is brought to you for free and open access by the School of Chemical and Pharmaceutical Sciences at ARROW@TU Dublin. It has been accepted for inclusion in Articles by an authorized administrator of ARROW@TU Dublin. For more information, please contact arrow.admin@tudublin.ie, aisling.coyne@tudublin.ie.

This work is licensed under a Creative Commons Attribution-Noncommercial-Share Alike 4.0 License

# Synthesis and structural characterizations of *ansa*-vanadabis(tricarbadecaboranyl) sandwich complexes

Ariane Perez-Gavilan,[†,*] Patrick J. Carroll[††] and Larry G. Sneddon[††,*]

[†]Maastricht Science Programme, Maastricht University, Maastricht 6211KW, The Netherlands and the [††]Department of Chemistry, University of Pennsylvania, Philadelphia, PA 19104-6323

* Corresponding authors.

E-mail addresses:

ariane.perez-gavilan@maastrichtuniversity.nl

lsneddon@sas.upenn.edu

*Dedicated to our friends Nancy and Russ Grimes on the occasion of Russ's 80th birthday*

**Abstract**

A new linked bis(tricarbadecaboranyl) dianion has been used to form the first examples of *ansa*-vanadabis(tricarbadecaboranyl) complexes. The $Li_2^+[6,6\text{-}(CH_2)_4\text{-}nido\text{-}(5,6,9\text{-}C_3B_7H_9)_2]^{2-}$ (**1**) dianion was produced by a carbon-insertion route involving the reaction of two equivalents of *arachno*-4,6-$C_2B_7H_{12}^-$ with adiponitrile. The reaction of **1** with $VCl_3$·THF produced two isomeric *ansa*-vanadabis(tricarbadecaboranyl) complexes, *ansa*-

(2',4-$(CH_2)_4$-)-*commo*-V-(1'-V-2',3',5'-$C_3B_7H_9$)(1-V-2,3,4-$C_3B_7H_9$) (**2**) and *ansa*-(2',4-$(CH_2)_4$-)-*commo*-V-(1'-V-2',3',4'-$C_3B_7H_9$)(1-V-2,3,4-$C_3B_7H_9$) (**3**). Crystallographic determinations showed that in both complexes a formal $V^{2+}$ ion is sandwiched between two tricarbadecaboranyl cages that are linked by the *ansa*-$(CH_4)_2$- group, but that the points of linker-attachment on the two cages are different. One cage of each complex has the linkage attached to the C2 cage-carbon, but in the other cage, a cage-atom rearrangement moved the C2 cage-carbon along with its attached -$(CH_4)_2$- linker to an adjacent 4-position. This rearrangement along with the long flexible -$(CH_4)_2$- linker enables the two cages in each complex to rotate into a perpendicular interlocking configuration that maximizes the bonding interaction with the metal, reduces unfavorable steric interactions between the two linked cages and encapsulates the vanadium inhibiting its interactions with other potential ligands. The isomeric structures of **2** and **3** differ as a result of their being formed from different combinations of the enantiomeric forms of the -$(CH_4)_2$-$C_3B_7H_9$ cages, with the C4 and C5' carbons on opposite sides of the tether in **2**, whereas in **3** the C4 and C4' carbons are on the same side.

Keywords: *ansa*-complex, *ansa*-vanadabis(tricarbadecaborane), *ansa*-metallocene, tricarbaborane, metallatricarbaborane, *ansa*-carborane

## Introduction

We have demonstrated that the 6-R-5,6,9-*nido*-$C_3B_7H_9^-$ (R = Me or Ph) [1, 2] tricarbadecaboranyl anions can function as cyclopentadienyl analogs with the tricarbadecaboranyl sandwich complexes exhibiting properties that are complimentary to their metallocene cousins [3]. For example, we previously synthesized [4] a range of different vanadabis(tricarbadecaboranyl) complexes V(Me-$C_3B_7H_9)_2$ sandwich complexes and demonstrated that, unlike the $Cp_2V$ [5] and $Cp^*_2V$ [6] vanadocenes, the vanadabis(tricarbadecaboranes) are both air and water stable, as well as unreactive toward coordination with additional ligands. In light of the unique properties imparted by tricarbadecaboranyl ligands, we have continued to explore the syntheses and properties of the tricarbadecaboranyl equivalents of other important classes of metallocene structure types.

*Ansa*-ligated metallocene [7] and metallacarboranyl complexes [8] are new and growing classes of stabilized sandwich complexes with constrained geometries that have found increasing uses as, for example, stereo-selective catalysts, chelating agents for metal separations and biomedical reagents. We recently reported [9] the synthesis of both the first linked cyclopentadienyl-tricarbadecaboranyl and bis(tricarbadecaboranyl) dianions and their use to form the first examples of *ansa*-ferratricarbadecaboranyl complexes. The short length of the -$(CH_2)_2$- linker used in the *ansa*-ferrabis(tricarbadecaboranyl) complexes inhibited coordination of the their two linked-cages in the most favorable interlocking configuration. In this paper, we report the synthesis of a new linked bis(tricarbadecaboranyl) dianion with a longer, four-carbon tether that facilitates optimal metal-cage bonding interactions, as illustrated by the use of this dianion to form the first *ansa*-vanadabis(tricarbadecaboranyl) complexes.

**Results and Discussion**

We earlier demonstrated that the carbon insertion method originally developed by Kang [1, 4], which employs the reaction of the *arachno*-4,6-$C_2B_7H_{12}^-$ anion with nitriles, could be used with succinonitrile to make the linked-cage [6,6-$(CH_2)_2$-*nido*-(5,6,9-$C_3B_7H_9)_2]^{2-}$ dianion [9]. In a similar fashion, the reaction of two equivalents of *arachno*-4,6-$C_2B_7H_{12}^-$ with adiponitrile produced a solution of the $Li_2^+$[6,6-$(CH_2)_4$-*nido*-(5,6,9-$C_3B_7H_9)_2]^{2-}$ (**1**) salt containing the longer 4-carbon linkage. The $^{11}$B NMR spectrum of the reaction solution at completion exhibited the seven resonance pattern that is highly characteristic of the 6-R-*nido*-5,6,9-$C_3B_7H_9^-$ anion and was similar to that observed for the previous [6,6-$(CH_2)_2$-*nido*-(5,6,9-$C_3B_7H_9)_2]^{2-}$ dianion. Because the tricarbadecaborane cage is enantiomeric, **1** is produced as a mixture of the two diastereomeric forms shown in **Scheme 1** resulting from the R+S and R+R (or S+S) combinations of the 6-R-*nido*-5,6,9-$C_3B_7H_9^-$ enantiomers. **1** was not isolated at this point, but was instead stored as a stock solution under $N_2$ until its further reaction.

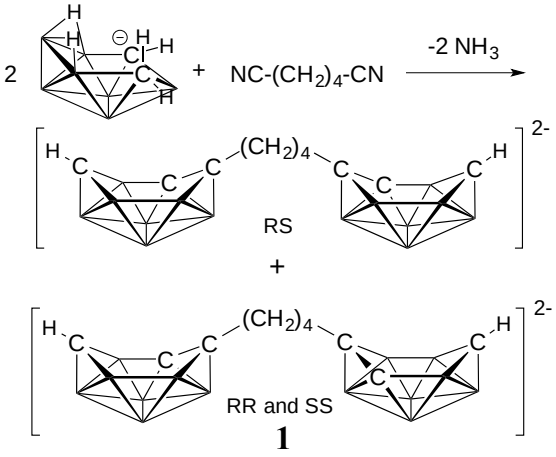


**Scheme 1.** Synthesis of $Li_2^+$[6,6-$(CH_2)_4$-*nido*-(5,6,9-$C_3B_7H_9)_2]^{2-}$ (**1**)

As depicted in **Scheme 2**, the 1:1 reaction of **1** with $VCl_3 \cdot THF$ in THF solution yielded, following purification by preparative TLC using a $CH_2Cl_2$ eluent, approximately equal amounts of two dark green crystalline solids.

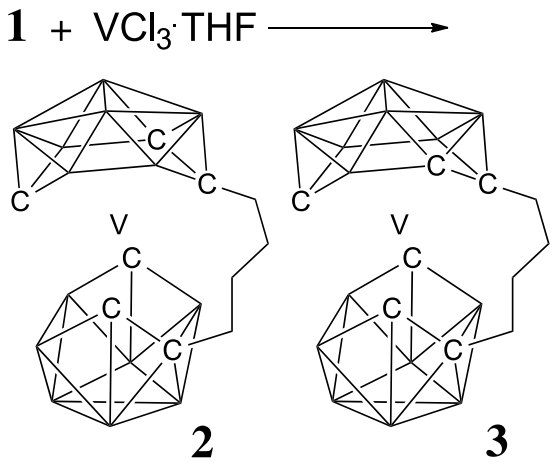


**Scheme 2.** Synthesis of *ansa*-complexes **2** and **3**.

As observed in the reactions to form the $V(Me\text{-}C_3B_7H_9)_2$ complexes, during the reaction to form **2** and **3**, reduction to V(II) occurred with the lower oxidation state stabilized by the highly electron-withdrawing tricarbadecaboranyl ligands [3, 4, 10]. Like the V(II) vanadocene complexes, $Cp_2V$ [5] and $Cp^*_2V$ [6], **2** and **3** are paramagnetic with a 15 electron count at the vanadium. However, unlike $Cp_2V$ and $Cp^*_2V$, which are high spin complexes with three unpaired electrons, Evan's method measurements indicated, as was observed for the untethered $V(Me\text{-}C_3B_7H_9)_2$ complexes [4], that **2** ($\mu_{eff}$ = 1.77) and **3** ($\mu_{eff}$ = 1.73) had only one unpaired electron. This difference in magnetism is again consistent with both the lower symmetry and stronger bonding properties of the tricarbadecaboranyl versus the Cp/Cp* ligands.

Owing to their paramagnetism, **2** and **3** could not be characterized with the aid of NMR; however, crystallographic determinations confirmed the *ansa*-structures shown in **Figures 1** and **2**.

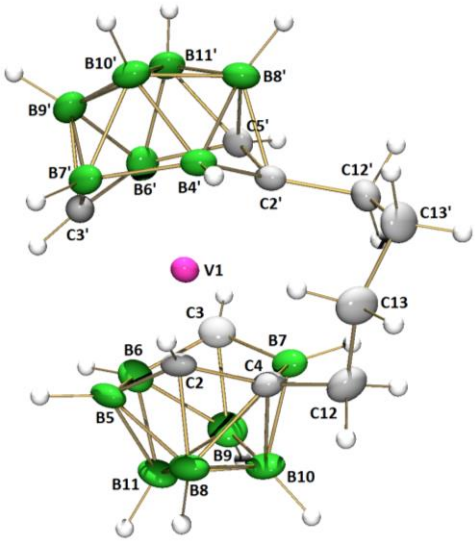


**Figure 1.** Crystallographically determined structure of **2**. Selected distances (Å) and angles (deg): V1–C2, 2.002(4); V1–C3, 2.105(8); V1–C4, 2.381(4); V1–B5, 2.364(8); V1–B6, 2.424(5); V1–B7, 2.439(6); V1–$(C4–B5–B6–B7)_{centroid}$, 1.810540(6); V1–$(C4'–B5'–B6'–B7')_{centroid}$, 1.75436(1); C2–B5, 1.601(8); B5–B6, 1.832(8); C3–B6, 1.571(12); C3–B7, 1.586(11); C4–B7, 1.736(6); C2–C4, 1.515(6); C4–C12, 1.527(5); V1–C2', 2.058(4); V1–C3', 1.999(4); V1–C5', 2.363(4); V1–B4', 2.355(6); V1–B6', 2.339(9); V1–B7', 2.362(9); C2'–B4', 1.594(6); B4'–B7', 1.856(14); C3'–B6', 1.589(8); C3'–B7', 1.576(12); C5'–B6', 1.724(7); C2'–C5', 1.516(5); C12'–C2', 1.532(5); C3–V1–C2, 102.0(2); C3'–V1–C2', 105.31(15); V1–C4–C12, 129.0(2).

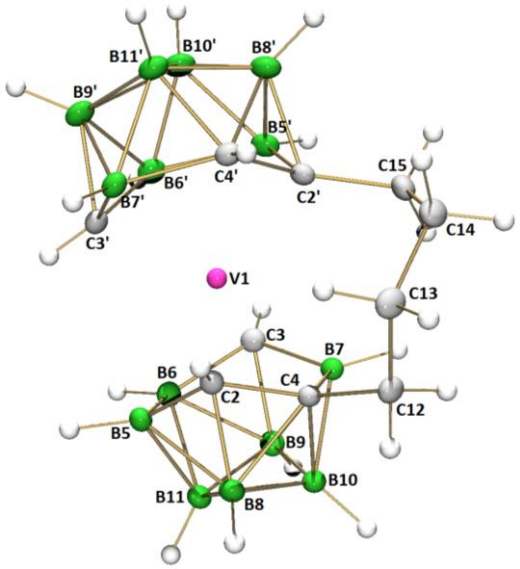


**Figure 2.** Crystallographically determined structure of **3**. Selected distances (Å) and angles (deg): V1–C2, 2.0478(9); V1–C3, 2.0425(9); V1–C4, 2.3784(9); V1–B5, 2.4180(11); V1–B6, 2.4207(11); V1–B7, 2.3696(10); V1–$(C4–B5–B6–B7)_{centroid}$, 1.8006(1); V1–$(C4'–B5'–B6'–B7')_{centroid}$, 1.7713(1); C2–B5, 1.5834(14); B5–B6, 1.8495(16); C3–B6, 1.5874(14); C3–B7, 1.5923(14); C4–B7, 1.7386(14); C2–C4, 1.5191(12); C4–C12, 1.5320(13); V1–C2', 2.0585(9); V1–C3', 2.0284(10); V1–C4', 2.3431(9); V1–B5', 2.3886(11); V1–B6', 2.3778(11); V1–B7', 2.3660(11); C2'–B5', 1.5948(15); B5'–B6', 1.8462(16); C3'–B6', 1.5923(14); C3'–B7', 1.5996(14); C4'–B7', 1.7282(14); C2'–C4', 1.5320(13); C15–C2', 1.5303(13); C3–V1–C2, 102.82(4); C3'–V1–C2', 105.24(4); V1–C4–C12, 127.56(6).

In both complexes, a formal $V^{2+}$ ion is sandwiched between two tricarbadecaboranyl ligands that are linked by the -$(CH_2)_4$- chain. The **2** and **3** structures differ only in the handedness of cages. Thus, as can be seen by comparing **Figures 1** and **2**, in compound **2**, the C4 and C5' cage-carbons are on opposite sides of the tether, whereas in **3** the C4 and C4' cage-carbons are on the same side. The vanadium in each complex is centered over the six-membered, puckered open faces of the two cages, with the C4–B5–B6–B7 and C4'(5')–B5'–B6'–B7' planes being nearly parallel, but slightly tilted away from the tether side (**2**: 5(2)$^o$, **3**: 5.3(3)$^o$). The shortest vanadium-cage distances are to the C2(2') and C3(3') carbons that are puckered toward the vanadium and these distances, as well as the V1–$(C4–B5–B6–B7)_{centroid}$ and V1–$(C4'(5')–B5'–B6'–B7')_{centroid}$ distances, are similar to those of the untethered V(Me-$C_3B_7H_9)_2$ complexes [4]. These centroid distances are significantly shorter than the V-Cp $_{centroid}$ distance (1.923 Å) in vanadocene [11].

Even though each of the $VC_3B_7$ cluster fragments in **2** and **3** have only 21 skeletal electrons, their cage structures appear identical to that of the 11-vertex *closo*-octadecahedral geometry framework expected for a 24 skeletal electron system, such as (1-$\eta^5$-$C_5H_5$)-*closo*-(2-$CH_3$-2,3,4-$C_3B_7H_9$)Fe. The absence of any cage distortions in **2** and **3** is consistent with the observation by Wade [12] that, as a result of their HOMO and LUMO orbitals not having degenerate levels, 11-vertex clusters have a unique ability to accommodate various electron counts in an octadecahedral framework.

In both **2** and **3**, the linker attachment points on their two cages are different. One cage of each complex has the linkage attached to the C2 cage-carbon, but in the other cage, a cage-atom rearrangement moved the C2 cage-carbon along with its attached -$(CH_4)_2$- linker to the adjacent 4-position. Such cage-carbon migrations have frequently been observed in many alkyl-

substituted metallatricarbadecaboranyl complexes, including the untethered V(Me-$C_3B_7H_9)_2$ complexes [4]. We have previously demonstrated [13] via $^{13}C$ labeling studies of the isomerization of (1-$\eta^5$-$C_5H_5$)-*closo*-(2-$CH_3$-2-*$^{13}C$*-2,3,4-$C_3B_7H_9$)Fe to its (1-$\eta^5$-$C_5H_5$)-*closo*-4-$CH_3$-4-*$^{13}C$*-2,3,4-$C_3B_7H_9$)Fe isomer that these isomerizations are consistent with a simple cage belt-rotation mechanism where the C2 cage-carbon moves to the adjacent 4 (or 5) position while retaining its exopolyhedral-substituent. Such a process could also readily account for the formation of **2** and **3**. Thus, as shown in **Scheme 3**, initial formation of the two isomeric *ansa*-(2',2-$(CH_2)_4$-)-*commo*-V-(1'-V-2',3',5'-$C_3B_7H_9$)(1-V-2,3,5-$C_3B_7H_9$) (top, left) and *ansa*-(2',2-$(CH_2)_4$-)-*commo*-V-(1'-V-2',3',4'-$C_3B_7H_9$)(1-V-2,3,5-$C_3B_7H_9$) (bottom right) complexes would result from reactions of $VCl_3$ with the R+S and R+R/S+S forms of **1**, respectively. As shown in the **Scheme**, the structure observed for **2** can then be derived from the *ansa*-(2',2-$(CH_2)_4$-)-*commo*-V-(1'-V-2',3',5'-$C_3B_7H_9$)(1-V-2,3,5-$C_3B_7H_9$) isomer by a simple rotation of its C5–C2–B4–B10–B11 belt, with C5 moving to the 2-position and the C2 carbon moving to the 4-position with its tether connection staying intact. In the same way, the structure of **3** can be generated from the *ansa*-(2',2-$(CH_2)_4$-)-*commo*-V-(1'-V-2',3',4'-$C_3B_7H_9$)(1-V-2,3,5-$C_3B_7H_9$) isomer by the rotation that moves the C2-substituted carbon to the 4-position. Further supporting the sequences outlined in **Scheme 3** is our previous observation that the (2',2-$(CH_2)_2$-)-*commo*-Fe-(1'-Fe-2',3',4'-$C_3B_7H_9$)(1-Fe-2,3,4-$C_3B_7H_9$) complex can likewise be converted to its *ansa*-(2',4-$(CH_2)_2$-)-*commo*-Fe-(1'-Fe-2',3',5'-$C_3B_7H_9$)(1-Fe-2,3,4-$C_3B_7H_9$) isomer [9].

The cage-carbon migration in combination with the longer -$(CH_2)_4$- linker allows the two cages in **2** and **3** to rotate to a perpendicular interlocking position, as measured by the dihedral angles between the C2–V1–C3 and C2'–V1–C3' planes in **2** (85.0(1)$^o$) and **3** (89.16(2)$^o$). This orientation maximizes the bonding interaction with the metal and prevents unfavorable steric

interactions between the two linked cages. This was the favored cage confirmation observed for the untethered (Me-$C_3B_7H_9)_2V$ isomers and results in encapsulation of the metal center thus inhibiting its further reactions with other potential reactants [4]. This orientation contrasts with those observed for the *ansa*-ferrabis(tricarbadecaboranyl) complexes *ansa*-(2',4-$(CH_2)_2$-)-*commo*-Fe-(1'-Fe-2',3',5'-$C_3B_7H_9$)(1-Fe-2,3,4-$C_3B_7H_9$) and *ansa*-(2',4-$(CH_2)_2$-)-*commo*-Fe-(1'-Fe-2',3',5'-$C_3B_7H_9$)(1-Fe-2,3,4-$C_3B_7H_9$) containing the 2-carbon linker where their shorter tethers force the cages into more eclipsed conformations with dihedral angles between their C2–Fe–C3 and C2'–Fe–C3' planes of only 64.04(5)$^o$ and 56.36(4)$^o$ [9].

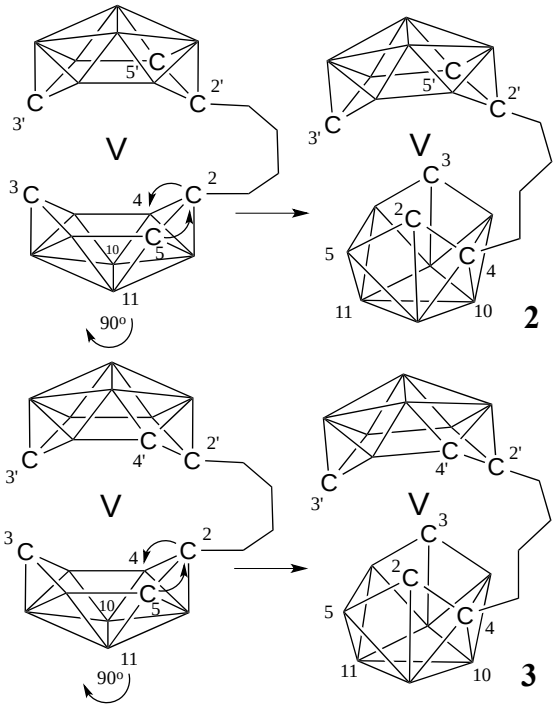


**Scheme 3.** Cage-carbon migration reactions by a belt-rotation mechanism leading to the formation of **2** and **3**.

In summary, the new linked-cage [6,6-$(CH_2)_4$-*nido*-(5,6,9-$C_3B_7H_9)_2$]$^{2-}$ dianion has been used to form the first examples of *ansa*-vanadabis(tricarbadecaboranyl) complexes. A cage-carbon rearrangement along with the long flexible -$(CH_4)_2$- linker enables the two cages in these complexes to rotate into a perpendicular interlocking configuration that maximizes the bonding interaction with the metal, reduces unfavorable steric interactions between the two linked cages and encapsulates the vanadium inhibiting its interactions with other potential reactants. These types of bis(tricarbadecaboranyl) dianions thus hold great promise for the syntheses of new families of highly stabilized *ansa*-sandwich compounds.

**Acknowledgments**

The National Science Foundation is gratefully acknowledged for both the support of this research (CHE-1011748) and for an instrumentation grant (CHE–0840438) that was used for the purchase of the X-ray diffractometer employed in these studies. The Maastricht Science Programme is gratefully acknowledged for the release time needed to conduct this research.

**Appendix A.** CCDC ???? (**2**) and CCDC ???? (**3**) contain the supplementary crystallographic data for the reported structures. These data can be obtained free of charge from The Cambridge Crystallographic Data Centre via www.ccdc.cam.ac.uk/data_request/cif.

## Experimental

*General Procedures and Materials:*

Unless otherwise noted, all reactions and manipulations were performed in dry glassware under nitrogen atmospheres using the high-vacuum or inert-atmosphere techniques described by Shriver [14].

The *arachno*-4,6-$C_2B_7H_{13}$ was prepared as previously reported [15]. $VCl_3$·THF (Strem), lithium hydride, and adiponitrile (Aldrich) were used as received. Tetrahydrofuran (THF) (Fisher) was freshly distilled from sodium benzophenone ketyl. Dichloromethane and diethyl ether (Fisher) were used as received.

$^{11}B$ NMR at 128.4 MHz was obtained on a Bruker DMX 400 spectrometer. The $^{11}B$ NMR chemical shifts are referenced to external $BF_3$·$OEt_2$ (0.00 ppm) with a negative sign indicating an upfield shift. The effective magnetic moments of the complexes were measured by using the Evans method [16]. High- resolution mass spectra using negative chemical ionization (NCI) were recorded on a Micromass Autospec Spectrometer. Infrared spectra were recorded on an ASI ReactIR 1000 FT-IR spectrometer. Preparative silica gel plates (1000 μm, Whatman) were used for chromatography. Melting points were obtained on a standard melting point apparatus and are uncorrected.

*Synthesis of $Li_2^+[6,6\text{-}(CH_2)_4\text{-}nido\text{-}(5,6,9\text{-}C_3B_7H_9)_2]^{2-}$ (**1**):*

LiH (20 mg, 2.6 mmol) and *arachno*-4,6-$C_2B_7H_{13}$ (300 mg, 2.6 mmol) were weighed into a Schlenk flask under $N_2$. Previously dried and distilled THF (10 mL) was added by syringe and the reaction was stirred at room temperature. The solution was monitored by NMR until ~97% complete. At this point, the lithium hydride was filtered off and adiponitrile (0.13 mL, 1.3

mmol) was added by syringe. The reaction mixture was stirred at reflux for 4 h until completion was observed via $^{11}$B NMR. The solution was then stored as a stock solution in the fridge until use. The approximate concentration of the stock solution and the yield (~92%, ~0.15 M) were determined by integrating the resonances in the $^{11}$B NMR spectrum of a $B_{10}H_{14}$ sample of known concentration and then comparing that value with the integrated value of the resonances of the stock solution.

**1**: $^{11}$B NMR (128.4 MHz, $CD_2Cl_2$, ppm, *J* = Hz) 6.6 (d, 124, 1B), 3.9 (d, 124, 1B), –5.8 (d, 124, 1B), –10.9 (d, 151, 1B), –13.3 (d, 124, 1B), –24.7 (d, 151, 1B), –31.9 (d, 138, 1B).

*Synthesis of ansa-(2',4-$(CH_2)_4$-)-commo-V-(1'-V-2',3',5'-$C_3B_7H_9$)(1-V-2,3,4-$C_3B_7H_9$) (**2**) and ansa-(2',4-$(CH_2)_4$-)-commo-V-(1'-V-2',3',4'-$C_3B_7H_9$)(1-V-2,3,4-$C_3B_7H_9$) (**3**):*

A THF solution of **1** (1.6 mL of a ~0.15 M solution, 0.24 mmol) was added to a Schlenk flask containing $VCl_3$·THF (187 mg, 0.5 mmol) under $N_2$. After stirring for 36 h at reflux, the reaction mixture was exposed to air and filtered through a short silica gel plug using $CH_2Cl_2$ and diethyl ether as eluents. The solvent was vacuum evaporated and the oily blue residue was re-dissolved in $CH_2Cl_2$ and chromatographed on a silica gel plate using a pure $CH_2Cl_2$ eluent to give two green bands, which were then extracted with $CH_2Cl_2$ to yield the two isomers:

**2**: ($R_f$ = 0.9); 15.4% yield (13 mg, 0.037 mmol); green; mp 193-196 ºC. NCI HRMS *m/z* for $C_{10}H_{26}B_{14}V$: calcd. 351.3545, fd. 351.3558; $\mu_{eff}$ = 1.77; IR: 2560 $cm^{-1}$ (br) B-H.

**3**: (Rf = 0.5), 14.2% yield (12 mg, 0.034 mmol); green; mp 171-174 ºC. NCI HRMS *m/z* for $C_{10}H_{26}B_{14}V$: calcd. 351.3545, fd. 351.3485; $\mu_{eff}$ = 1.73; IR: 2580 $cm^{-1}$ (br) B-H

*Crystallographic Procedures:*

Single crystals were grown through slow solvent evaporation from dichloromethane solutions. X-ray intensity data were collected on a Bruker APEXII CCD diffractometer employing graphite-monochromated Mo-$K_\alpha$ radiation ($\lambda$=0.71073 Å). The structures were solved by direct methods (SIR97) [17]. Refinement was by full-matrix least squares based on $F^2$ using SHELXL-97 [18]. All reflections were used during refinement (values of $F^2$ that were experimentally negative were replaced with $F^2 = 0$). Non-hydrogen atoms were refined anisotropically, cage hydrogen atoms were refined isotropically, and all other hydrogen atoms were refined using a riding model. Crystal and refinement data are given in **Table 1**. Selected bond distances and angles are given in the figure captions.

**Table 1.** Crystallographic Data Collection and Structure Refinement Information.

| | **2** | **3** |
|---|---|---|
| Empirical Formula | $C_{10}B_{14}H_{26}V$ | $C_{10}B_{14}H_{26}V$ |
| Formula weight | 348.59 | 348.59 |
| Crystal class | orthorhombic | monoclinic |
| Space group | Pbcn | $P2_1/n$ |
| Z | 4 | 4 |
| *a*, Å | 13.2482(7) | 9.7439(3) |
| *b*, Å | 13.0650(6) | 12.7064(4) |
| *c*, Å | 10.5990(6) | 15.0961(4) |
| *β*, deg | | 98.9700(10) |
| V, $Å^3$ | 1834.56(17) | 1846.19(9) |
| $D_{calc}$, $g/cm^3$ | 1.262 | 1.254 |
| $\mu$, $mm^{-1}$ | 0.528 | 0.525 |
| $\lambda$, Å (Mo-$K_\alpha$) | 0.71073 | 0.71073 |
| Crystal size, mm | 0.20 x 0.14 x 0.03 | 0.45 x 0.32 x 0.25 |
| F(000) | 716 | 716 |
| 2θ angle, deg | 4.38–55.08 | 4.22–55.04 |
| Temperature, K | 100(1) | 100(1) |
| *hkl* collected | $-17 \le h \le 17$<br>$-16 \le k \le 17$<br>$-13 \le l \le 13$ | $-12 \le h \le 12$<br>$-16 \le k \le 16$<br>$-19 \le l \le 19$ |
| No. meas reflns | 41816 | 49199 |

| | | |
|---|---|---|
| No. unique reflns | 2115 [$R_{int}$ = 0.0460] | 4255 [$R_{int}$ = 0.0176] |
| No. parameters | 223 | 331 |
| $R^a$ indices (all data) | $R_1$ = 0.0420, $wR_2$ = 0.0798 | $R_1$ = 0.0237, $wR_2$ = 0.0635 |
| $R^a$ indices ($F > 2\sigma$) | $R_1$ = 0.0294, $wR_2$ = 0.0749 | $R_1$ = 0.0223, $wR_2$ = 0.0616 |
| GOF[b] | 1.088 | 0.921 |
| Final difference peaks, e/ Å$^3$ | 0.159 | 0.365 |

[a] $R_1 = \sum||F_o|-|F_c||/\sum|F_o|$; $wR_2 = \{\sum w(F_o^2-F_c^2)^2/\sum w(F_o^2)^2\}^{1/2}$ [b] GOF = $\{\sum w(F_o^2- F_c^2)^2/(n - p)\}^{1/}$

**References**


[1] S.O. Kang, G.T. Furst, L.G. Sneddon, Inorg. Chem. 28 (1989) 2339–2347.

[2] B.M. Ramachandran, P.J. Carroll, L.G. Sneddon, Inorg. Chem. 43 (2004) 3467–3474.

[3] See for example: (a) C.A. Plumb, P.J. Carroll, L.G. Sneddon, Organometallics 11 (1992) 1665–1671. (b) C.A. Plumb, P.J. Carroll, L.G. Sneddon, Organometallics 11 (1992) 1672–1680. (c) B.A. Barnum, P.J. Carroll, L.G. Sneddon, Inorg. Chem. 36 (1997) 1327–1337. (d) B.M. Ramachandran, S.M. Trupia, W.E. Geiger, P.J. Carroll, L.G. Sneddon, Organometallics 21 (2002) 5078–5090. (e) B.M. Ramachandran, Y.Wang, S.O. Kang, P.J. Carroll, L.G. Sneddon, Organometallics 23 (2004) 2989–2994.

[4] M.D. Wasczak, Y. Wang, A. Garg, W.E. Geiger, S.O. Kang, P.J. Carroll, L.G. Sneddon, J. Am. Chem. Soc. 123 (2001) 2783–2790.

[5] (a) P. Royo, E. Ryan, in Metallocenes: Synthesis, Reactivity, Applications; A. Togni, R.L. Halterman, Eds.; Wiley-VCH: New York (1998) Vol. 1, pp 321-414. (b) T.A. Jackson, J.

Krzystek, A. Ozarowski, G.B. Wijeratne, B.F. Wicker, D.J. Mindiola, J. Telser, Organometallics 31 (2012) 8265–8274.

[6] J.L. Robbins, N. Edelstein, B. Spencer, J.C. Smart, J. Am. Chem. Soc. 104 (1982) 1882–1893.

[7] For some general references on the properties of *ansa*-Cp complexes, see: (a) P.J. Shapiro, Coord. Chem. Rev. 231 (2002) 67–81. (b) S. Prashara, A.A. Nolo, A. Otero, Coord. Chem. Rev. 250 (2006) 133–154. (c) B. Wang, Coord. Chem. Rev. 250 (2006) 242–258. (d) G. Erker, Macromol. Symp. 236, (2006) 1–13.

[8] For some examples of *ansa*-metalladicarbaboranyl complexes see: (a) Y. Wang, H. Wang, H-W. Li, Z. Xie, Organometallics 21 (2002) 3311–3313. (b) Z. Xie, Accts. Chem. Res. 36 (2003) 1–9. (c) Y. Wang, D. Liu, H-S. Chan, Z. Xie, Organometallics 27 (2008) 2825–2832. (d) D. Liu, Y. Wang, H-S. Chan, Y. Tang, Z. Xie, Organometallics 27 (2008) 5295–5302. (e) M-M. Sit, H-S. Chan, Z. Xie, Organometallics 28, (2009) 5998–6002.

[9] B. Gleeson, P.J. Carroll, L.G. Sneddon, J. Am. Chem. Soc. 135 (2013) 12407–12413.

[10] (a) A. Nafady, R. Butterick III, M.J. Calhorda, P.J. Carroll, D. Chong, W.E. Geiger, L.G. Sneddon, Organometallics 26 (2007) 4471–4482. (b) M. Stewart, R. Butterick III, L.G. Sneddon, Y. Matsuo, G.E. Geiger, Inorg. Chim. Acta 364 (2010) 251–254.

[11] (a) M.Y. Antipin, K.A. Lyssenko, R. Boese, J. Organomet. Chem. 508 (1996**)** 259–262. (b) R.D. Rogers, J.L. Atwood, D. Foust, M.D. Rausch, J. Cryst. Mol. Struc. 11 (1981) 183–188.

[12] (a) M.E. O'Neill, K.J. Wade, Mol. Struct. 103 (1983) 259–268. (b) M.E. O'Neill, K.J. Wade, Polyhedron 2 (1984) 199–212. (c) R.E. Mulvey, M.E. O'Neill, K.J. Wade, R. Snaith, Polyhedron 5 (1986) 1437–1447.

[13] C.A. Plumb, P.J. Carroll, L.G. Sneddon, Organometallics 11 (1992) 1681–1685.

[14] D.F. Shriver, M.A. Drezdzon, The Manipulation of Air-Sensitive Compounds, 2nd ed.; Wiley: New York, (1986)

[15] (a) M.F. Hawthorne, D.C. Young, P.M. Garrett, D.A. Owen, S.G. Schwerin, F.N. Tebbe, P.A. Wegner, J. Am. Chem. Soc. 90 (1968) 862–868. (b) P.M. Garrett, T.A. George, M.F. Hawthorne, Inorg. Chem. 8 (1969) 2008–2009.

[16] (a) D.F. Evans, J. Chem. Soc. (1959) 2003−2005. (b) J. Loliger, R.J. Scheffold, J. Chem. Educ. 49 (1972) 646−647. (c) C.J. Piguet Chem. Educ. 74 (1997) 815−816.

[17] *SIR97*: A. Altomare, M.C. Burla, M. Camalli, M. Cascarano, C. Giacovazzo, A. Guagliardi, A. Moliterni, G.J. Polidori, R.J. Spagna, Appl. Cryst. 32 (1999) 115–119.

[18] SHELXTL version 6.14: Bruker AXS Inc., Madison, WI, USA.

## Graphic for Table of Contents

## Graphical Abstract Synopsis

The synthesis and structural characterizations of new *ansa*-vanadabis(tricarbadecaboranyl) complexes has been achieved, with the flexible 4-carbon cage-linker in these complexes facilitating a cage-carbon migration that allows the cages to adopt a favorable interlocking position encapsulating the vanadium.

## Highlights

- Synthesis and structural characterizations of the first *ansa*-vanadabis(tricarbadecaboranyl) complexes
- The *ansa*-vanadabis(tricarbadecaboranes) are paramagnetic with one unpaired electron
- Cage-carbon migration in the *ansa*-vanadabis(tricarbadecaboranes) enhances the tricarbadecaboranyl bonding configuration
- Flexible linker allows for an encapsulation of the metal center that inhibits its interactions with other potential reactants